Preparation of Bead-Tailed Actin Filaments: Estimation of the Torque Produced by the Sliding Force in an In Vitro Motility Assay

Naoya Suzuki,* Hidetake Miyata,* Shin'ichi Ishiwata,‡ and Kazuhiko Kinosita, Jr.*
*Department of Physics, Faculty of Science and Technology, Keio University, 3–14-1, Hiyoshi, Kohoku-ku, Yokohama 223, Japan; and ‡Department of Physics, School of Science and Engineering, Waseda University, 3–4-1, Okubo, Shinjuku-ku, Tokyo 169, Japan

ABSTRACT By coating covalently the surface of a polystyrene bead (diameter = 1 μm) with gelsolin, we have succeeded in attaching the bead selectively at the barbed end of an actin filament and forming a 1:1 bead-actin filament complex. On a layer of heavy meromyosin on a nitrocellulose-coated coverglass, this bead-actin filament complex slid smoothly, trailing the bead at its end. Therefore we called this preparation "bead-tailed" actin filaments. The sliding velocity was indistinguishable from that of nonbeaded filaments. With use of this system, we tried to detect the axial rotation (rotation around the filament axis) in a sliding actin filament. Although a single bead at the tail end did not serve as the marker for the axial rotation, we occasionally found another bead bound to the tail bead. In this case, the orientation of the bead-aggregate could be followed continuously with a video monitor while the filament was sliding over heavy meromyosin. We observed that actin filaments slid over distances of many tens of micrometers without showing a complete turn of the bead-aggregates. On the basis of the calculation of rotational friction drag on the bead-aggregate, we estimate that the rotational component of the sliding force and the torque produced on a sliding actin filament (length ≤10 μm) did not accumulate >1 pN and 5 pN · nm, respectively, in the present system of randomly oriented heavy meromyosin lying on a nitrocellulose film without an external load.

INTRODUCTION

To reveal the molecular mechanisms of muscle contraction and cell motility, much attention has been focused on in vitro motility assays (Harada et al., 1990; Huxley, 1990; Vale and Goldstein, 1990; Kron et al., 1991). Recently, several new systems that combine the in vitro motility assays with an apparatus for the simultaneous measurement of nanometer movements (Gelles et al., 1988; Svoboda et al., 1993; Block and Svoboda, 1995) and piconewton forces have been developed (Yanagida et al., 1993; Vale, 1994; Yanagida and Ishijima, 1995). In most of these systems, a bead is used as the handle for trapping with optical tweezers (Ashkin, 1992) and as the reporter of nanometer movements (Kuo and Sheetz, 1993; Svoboda et al., 1993; Finer et al., 1994, 1995; Miyata et al., 1994, 1995; Saito et al., 1994; Svoboda and Block, 1994; Coppin et al., 1995). In actomyosin motility assays, two beads coated with *N*-ethylmaleimide-modified myosin have been bound laterally to an actin filament (Finer et al., 1994, 1995; Saito et al., 1994; Molloy et al., 1995).

We describe here a method to attach a bead selectively to the rear end (barbed end) of an actin filament. The rear end-bound bead provides a relatively convenient means of measuring nanometer movements and piconewton forces with a single optical trap (Miyata et al., 1994, 1995; Nishizaka et al., 1995a,b) compared with the laterally bound beads with two optical traps (Finer et al., 1994, 1995; Saito et al., 1994; Molloy et al., 1995). To make beads designed to be bound to the barbed end of actin filaments, we used gelsolin. Gelsolin has the Ca^{2+}-dependent activity of severing an actin filament, capping the barbed end of the actin filament, and forming a polymerization nucleus as the complex with two actin monomers (Isenberg, 1991). When gelsolin was covalently bound to polystyrene beads (diameter = 1 μm) with EDC or glutaraldehyde, the coated bead was bound specifically to one end of an actin filament. The bead-binding actin filament slid smoothly in an in vitro motility assay, trailing the bead at its end as expected. Therefore, we called this preparation "bead-tailed" actin filaments.

As an application of the bead-tailed actin filaments, we attempted to detect the axial rotation (rotation around the filament axis) in a sliding actin filament. Here we used the tail beads as a marker of the axial rotation. Because an actin filament has a helical structure, the vector of the sliding force may be tilted against the long axis of the filament, and the sliding force has not only a translational component but also a rotational component. In the case of a microtubule and 14S dynein, the axial rotation of the microtubule was directly observed as the rotation of an axoneme attached to the rear end of the microtubule (Vale and Toyoshima, 1988). In the case of an actin filament and myosin, the axial rotation was indicated as a superhelix and a supercoil of the

Received for publication 10 April 1995 and in final form 5 October 1995.

Address reprint requests to Dr. K. Kinosita, Jr., Department of Physics, Faculty of Science and Technology, Keio University, 3–14-1, Hiyoshi, Kohoku-ku, Yokohama 223, Japan. Tel.: 81-45-563-1141, ext. 3975; Fax: 81-45-563-1761.

N. Suzuki's present address: Department of Physics, School of Science, Nagoya University, Furo-cho, Chikusa-ku, Nagoya 464–01, Japan.

Abbreviations used: HMM, heavy meromyosin; BSA, bovine serum albumin; EDC, 1-ethyl-3-[3-(dimethylamino)propyl]carbodiimide; MOPS, 3-morpholinopropanesulfonic acid; TMR, tetramethylrhodamine; DTT, dithiothreitol.

0006-3495/96/01/401/08 $2.00

actin filament (Tanaka et al., 1992; Nishizaka et al., 1993). However, we could not observe a complete turn of the tail beads. This suggests that the accumulated torque is not very high, at least in a usual in vitro motility assay system.

MATERIALS AND METHODS

Preparation of proteins

Acetone-dried powder of rabbit skeletal muscle was prepared according to the method of Ebashi and Maruyama (1965). Actin was extracted and purified by the method of Spudich and Watt (1971). Myosin was prepared from rabbit skeletal white muscle by the method of Perry (1955), with a slight modification described by Holtzer and Lowey (1959). HMM was prepared by α-chymotryptic digestion of myosin as described by Weeds and Taylor (1975). Gelsolin was purified from calf plasma by the method of Funatsu et al. (1990) or Kurokawa et al. (1990). HMM and gelsolin were stored in liquid nitrogen. Protein concentrations were determined spectrophotometrically using the extinction coefficients, $A^{1\%}_{1cm} = 6.3$ at 290 nm for actin (Houk and Ue, 1974), 6.0 at 280 nm for HMM (Margossian and Lowey, 1978), 6.6 at 280 nm for BSA (A4378; Sigma, St. Louis, MO), and $A^{mM}_{1cm} = 117$ at 280 nm for gelsolin (Weber et al., 1991). The absorption was corrected for light scattering using the apparent absorption at 320 nm. The molecular weights of proteins were taken as 42,000 for actin, 350,000 for HMM, 83,000 for gelsolin, and 67,000 for BSA.

TMR-labeled BSA was prepared as follows. TMR-maleimide (T-489; Molecular Probes, Eugene, OR) dissolved in *N,N*-dimethylformamide (DMF) was added to BSA solution (~3 mg/ml in 0.1 M KCl and 20 mM MOPS (pH 7.0)) in a molar ratio 3–4:1. The mixture was incubated for 6 h at 0°C in the dark. The reaction was then stopped by adding DTT (141–12; Nacalai Tesque, Kyoto, Japan) to 2 mM. The mixture was dialyzed and applied to a column of Sephadex G-25 (Pharmacia LKB, Uppsala, Sweden). Approximately 70–80% of BSA was labeled by this method.

Gelsolin-coated beads

Covalent coupling of gelsolin to carboxylated polystyrene beads was carried out basically according to the recommended protocol of Polysciences (Warrington, PA), with a slight modification as follows: 0.5 ml of a beads suspension (2.5% carboxylated polystyrene beads, diameter = 1 μm, no. 08226; Polysciences) was placed in a sample tube (1.5 ml capacity). The beads were washed four times with 0.1 M sodium carbonate buffer (pH 9.6) by 5-min centrifugations at 10,000 rpm (TL100, TLA100.3 rotor with an adapter for the sample tube; Beckman, Palo Alto, CA). The beads were then washed four times with 20 mM sodium phosphate buffer (pH 4.5). The beads were resuspended in 0.625 ml of 20 mM sodium phosphate buffer (pH 4.5) and sonicated for 1 min by dipping the sample tube into a sonication bath (Sun cleaner 40kHz; Sun Electron, Tokyo, Japan). EDC (348–0363; Dojindo Laboratories, Kumamoto, Japan) was dissolved to 2% (w/v) in 20 mM sodium phosphate buffer (pH 4.5), and 0.625 ml of the solution was added to the beads suspension. The suspension was mixed continuously and gently for 3.5 h at room temperature. The beads were collected with centrifugation at 10,000 rpm for 7 min and washed four times with 0.1 M borate buffer (pH 8.5). The beads were suspended in 0.7 ml of solution A containing 0.1 M borate buffer (pH 8.5), 0.1 mM $CaCl_2$, and 0.1 mM ATP (519979; Boehringer Mannheim, Mannheim, Germany) and sonicated for 30 s. Four hundred micrograms of proteins (320 μg BSA, 40 μg TMR-labeled BSA, 20 μg G-actin, and 20 μg gelsolin) dissolved in 0.5 ml of solution A was added to the beads suspension. The suspension was mixed continuously and gently for 8–10 h at room temperature in the dark. To stop the reaction, 50 μl of 0.25 M ethanolamine (012–12455; Wako Pure Chemical Industries, Osaka, Japan) was then added and mixed gently for 30 min. The beads were collected with centrifugation at 10,000 rpm for 7 min and resuspended in 1.2 ml of 10 mg/ml BSA in solution A. After sonication for 30 s, the suspension was gently mixed for 30 min. The beads were then washed three times with 10 mg/ml BSA in solution A. The beads were resuspended in 1 ml of a stock solution (150 mM NaCl, 20 mM sodium phosphate buffer (pH 7.4), 0.1 mM $CaCl_2$, 0.1 mM ATP, 10 mg/ml BSA, 5% (v/v) glycerol, and 0.1% (w/v) NaN_3) and stored at 0°C in the dark. The coated beads were usable for about 6 months. In the case of labeling beads of 0.5 μm diameter (no. 09836; Polysciences), three points were altered: centrifugation speed was 17,000 rpm, and 2.6% (w/v) EDC and 500 μg of total protein (with the same mixing ratio (w/w) as described above) were used.

Covalent coupling of gelsolin to amino polystyrene beads was also carried out basically according to the recommended protocol of Polysciences, with a slight modification as follows: 1 ml of a beads suspension (2.5% amino polystyrene beads, diameter = 1 μm, no. 17010; Polysciences) was placed in a sample tube. The beads were washed four times by 8-min centrifugations at 10,000 rpm with PBS containing 0.15 M NaCl and 20 mM sodium phosphate buffer (pH 7.4). The beads were mixed in 1.2 ml of 8% (v/v) glutaraldehyde (EM grade, 071-02031; Wako Pure Chemical Industries) in PBS and sonicated for 30 s. The suspension was mixed continuously and gently for 8 h at room temperature. The beads were then washed five times with PBS. In this washing process, the beads were sonicated for 30 s before each centrifugation. The beads were resuspended in 0.7 ml of solution B (0.15 M NaCl, 20 mM sodium phosphate buffer (pH 7.4), 0.1 mM ATP, and 0.1 mM $CaCl_2$) and sonicated for 30 s. Four hundred fifty micrograms of proteins (350 μg BSA, 50 μg TMR-labeled BSA, 25 μg G-actin, and 25 μg gelsolin) dissolved in 0.5 ml of solution B was added to the beads suspension. The suspension was mixed continuously and gently for 4.5 h at room temperature in the dark. The beads were collected with centrifugation at 10,000 rpm for 10 min. To stop the reaction, 1.2 ml of 0.5 M ethanolamine was added to the beads, and the suspension was sonicated for 30 s and mixed gently for 40 min. The beads were collected with centrifugation at 10,000 rpm for 10 min and resuspended in 1.2 ml of 10 mg/ml BSA in solution B. After sonication for 30 s, the suspension was gently mixed for 30 min. The beads were then washed three times with 10 mg/ml BSA in solution B. The beads were suspended in 1 ml of the stock solution and stored at 0°C in the dark. The coated beads were usable for about 6 months.

Bead-tailed actin filament

The gelsolin-coated beads stock (0.1 ml) was transferred into a sample tube, and 0.1 ml of solution C (25 mM imidazole-HCl (pH 7.4), 25 mM KCl, 4 mM $MgCl_2$, 0.1 mM $CaCl_2$, 0.1 mM ATP, 1 mM DTT, and 0.04% NaN_3) was added and sonicated for 30 s. The suspension was centrifuged at 6000 rpm for 4 min in a microcentrifuge. The beads were washed four times (six times for amino beads) with 0.2 ml of solution C. The beads were resuspended in 40 μl of solution C, and 10 μl of 10 μM F-actin labeled with TMR-phalloidin (Molecular Probes) (Yanagida et al., 1984) was added to the suspension. After gentle mixing, the suspension was incubated overnight at 0°C in the dark. The suspension was then diluted 1:50 with 2 mg/ml BSA in solution C and incubated for more than 2 h at 0°C. The diluted suspension was diluted further with a motility assay solution and used in an in vitro motility assay described below.

In vitro motility assay

The motility assay system we used was the same as that used by Kron et al. (1991), except for a slight modification as follows. We used Ca^{2+}- containing solutions: CaAB (25 mM imidazole-HCl (pH 7.4), 25 mM KCl, 4 mM $MgCl_2$, 0.1 mM $CaCl_2$, 1 mM DTT, and 0.04% (w/v) NaN_3), CaAB/BSA (2 mg/ml BSA in CaAB), CaAB/BSA/GOC (0.03 mg/ml catalase (C-10; Sigma), 0.15 mg/ml glucose oxidase (G-2133; Sigma), and 4.5 mg/ml glucose in CaAB/BSA), and CaAB/BSA/GOC/ATP (2 mM ATP in CaAB/BSA/GOC). We prepared a nitrocellulose-coated coverglass as follows: 2% collodion in isoamyl acetate (Ohken Industry, Tokyo, Japan) was diluted to 0.1% (v/v) in isoamyl acetate (019–03636; Wako Pure Chemicals Industries). Drops of diluted collodion were applied over a coverglass

(24 × 36 mm). The coverglass was tilted, the excess collodion was absorbed with a piece of filter paper, and the coverglass was air-dried. An experimental flow cell (depth = ~100 μm) was made of the collodion-coated coverglass and a noncoated coverglass (18 × 18 mm). We infused 90 μl of ~30 μg/ml HMM solution into the flow cell from one side, and immediately applied 90 μl of 0.5 mg/ml BSA in CaAB from the same side.

Observation system

TMR-labeled actin filaments and beads were observed with an inverted fluorescence microscope (TMD; Nikon, Tokyo, Japan) equipped with epifluorescence optics, an NCF Fluor DL ×100 objective (oil immersion, N.A. = 1.3; Nikon), a 100-W mercury arc lamp, and a G-2A filter cassette (Nikon). Fluorescence images were recorded on a videotape with an image intensifier (KS-1381; Video Scope, Washington, DC), a CCD camera (CCD-72; DageMTI, Michigan, IN), and a video recorder (S-VHS type; A-VS1 Toshiba or NV-FS1000 National, Tokyo, Japan). Movements were analyzed using a digital image processor (C2000; Hamamatsu Photonics, Hamamatsu, Japan).

RESULTS

Bead-tailed actin filaments

We used EDC for carboxylated beads and glutaraldehyde for amino beads as cross-linkers between gelsolin and beads. In both cases, we succeeded in preparing bead-tailed actin filaments. The results described below were essentially the same for both preparations.

We optimized two parameters in preparing the gelsolin-coated beads. One was the weight percentage of gelsolin to total protein (w/w) in the protein solution mixed with the activated beads. We used gelsolin as a 1:2 complex with monomeric actin; we maintained a 1:1 weight ratio of actin to gelsolin in all protein solutions. When the percentage was 50% (maximum percentage we examined, i.e., activated beads were mixed with the protein solution containing actin and gelsolin without BSA), many actin filaments bound to a single bead. When the percentage was too low (<1%), actin filaments scarcely bound to the beads. To maximize the number of actin filaments carrying a single bead, we usually adjusted the amount to several percent. However, this parameter depended on the age of gelsolin. With freshly prepared gelsolin, 1–2% was optimum. With aging of the gelsolin, the ability to bind the actin filament declined.

The other parameter was the weight percentage of TMR-labeled BSA to the total protein in the protein solution. The beads were visualized by staining them with TMR-labeled BSA, whereas actin filaments were labeled with TMR-phalloidin. The fluorescence brightness of the two should be approximately the same. This was achieved when the weight percentage was ~10%.

Fig. 1 shows the fluorescence images of the bead-tailed actin filaments in a rigor state. There were three types of bead-tailed actin filaments. The major type was a single actin filament carrying a single bead (Fig. 1 *a*). Another was a single actin filament carrying double (or more) beads (Fig. 1 *b*). We used this type of bead-tailed actin filaments to detect the axial rotation of a sliding actin filament. The bead-aggregate served as an asymmetric marker of the rotation around the filament axis. The last type was a single bead to which two (or more) actin filaments were bound (Fig. 1 *c*).

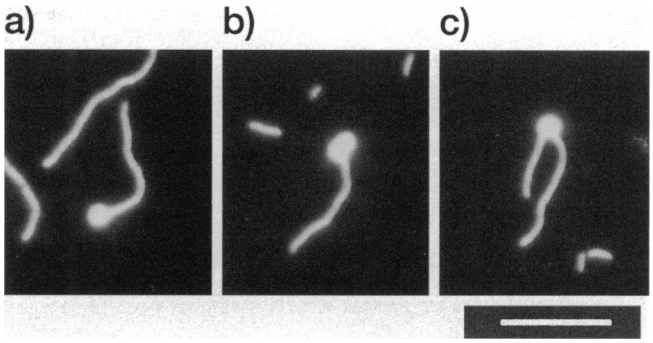

FIGURE 1 Fluorescence images of three types of bead-tailed actin filaments in a rigor state. Type (*a*), a single bead-tailed actin filament; type (*b*), a double bead-tailed actin filament; type (*c*), a single bead-tailed double actin filament. The diameter of the bead was 1.16 μm. Bar, 10 μm.

To confirm the specific binding of actin filaments to gelsolin on the beads, we performed two control experiments. In one, beads were covalently coated with BSA alone; in the other, the gelsolin-coated beads were mixed with F-actin without Ca^{2+} (1 mM EGTA was added to CaAB). In both cases, actin filaments were scarcely bound to the beads.

Sliding bead-tailed actin filaments

If the beads themselves have some nonspecific interaction with the HMM-coated glass surface, sliding of bead-tailed actin filaments must be obstructed. Unfortunately, the gelsolin-coated beads we prepared bound to the HMM-coated glass surface in the solution CaAB (in the rigor state without BSA). From the observations that addition of ATP did not detach the binding beads and the binding was suppressed by addition of BSA, we concluded that this binding was caused by nonspecific interaction (not by the specific interaction between actin on the beads and HMM coated on the glass). We found that the addition of BSA at 2 mg/ml was sufficient to reduce this nonspecific interaction to a negligible level. Therefore, all of the solutions for the sliding experiment contained 2 mg/ml BSA.

Fig. 2 shows the fluorescence images of a sliding bead-tailed actin filament. The bead-tailed actin filament slid smoothly, trailing the bead at its end. The sliding speed of the bead-tailed actin filaments was indistinguishable from that of the nonbeaded filaments (Fig. 3). This suggests that the trailing bead applied only a negligible load to the sliding actin filament.

When two actin filaments were bound to a single bead, each filament slid in its own direction. The two actin filaments formed a straight line, in opposite directions, and a pulling contest began between the opposing actin filaments (Fig. 4 *a*). When more than two actin filaments were bound to a single bead, all filaments slid away from the bead and

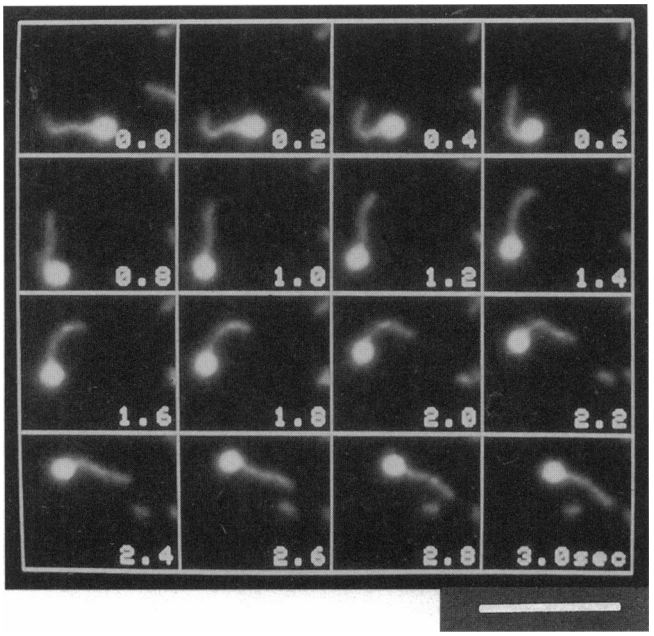

FIGURE 2 Fluorescence images, at 0.2-s intervals, of a sliding single bead-tailed actin filament in the in vitro motility assay (see Materials and Methods). The bead-tailed actin filament slid smoothly, trailing the bead at its end. The diameter of the bead was 1.16 μm. Bar, 10 μm.

were radially straightened from the bead (Fig. 4 *b*). These observations indicate that every actin filament bound to the gelsolin-coated bead had the same polarity; it was always the barbed end that was anchored to the bead.

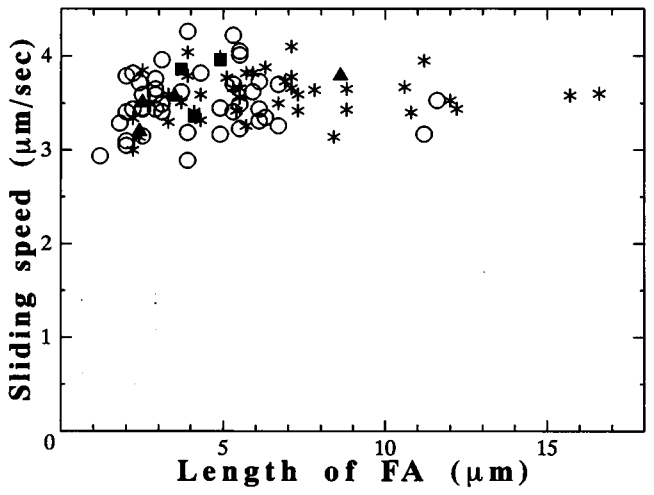

FIGURE 3 Sliding speeds of bead-tailed actin filaments and non-beaded actin filaments in the in vitro motility assay (see Materials and Methods) at 24°C. The diameter of the bead was 1.16 μm. The average sliding speeds ± SD (n = number of data, average length of actin filaments ± SD) were 3.59 ± 0.25 μm/s (n = 41, 6.60 ± 3.45 μm) for nonbeaded actin filaments (*asterisks*), 3.51 ± 0.32 μm/s (n = 43, 4.25 ± 2.25 μm) for single bead-tailed actin filaments (○), 3.52 ± 0.24 μm/s (n = 4, 4.25 ± 2.94 μm) for double bead-tailed actin filaments (▲), and 3.73 ± 0.32 μm/s (n = 3, 4.23 ± 0.61 μm) for triple bead-tailed actin filaments (■).

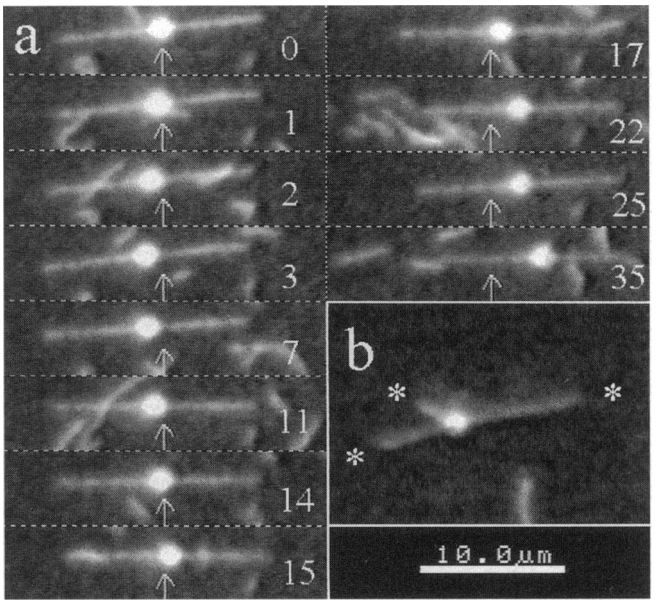

FIGURE 4 Single bead-tailed multiple actin filaments having the same polarity. (*a*) When two actin filaments were bound to a single bead, each filament pulled the bead. The two actin filaments formed a straight line, in opposite directions, and a pulling contest began between the opposing filaments. The arrows indicate the starting position of the pulling contest. The numbers are the elapsed time from the start of the pulling contest in seconds. (*b*) When three actin filaments were bound to a single bead, each filament (indicated by the *asterisks*) pulled the bead and was radially straightened from the bead. The diameter of the bead was 1.16 μm. Bar, 10 μm.

Attempt to detect the rotational motion during sliding

To detect the rotation of an actin filament around its long axis, we observed the sliding of the bead-tailed actin filaments. The orientation of the bead-aggregate (Fig. 5 *a*) was continuously followed by using a video monitor. The orientation fluctuated as seen in Fig. 5 *b*, but the fluctuations failed to accumulate into a turn. We observed a total of 58 filaments, 47 with double beads and 11 with triple beads, each for a continuous period of ~1 min. The total observation period was >1 h, corresponding to a total sliding distance of >12,000 μm. In these continuous runs, the bead-aggregate did not show a continuous rotation or a complete turn as an accumulation of fluctuations. Because of the quenching of fluorescence, the longest continuous observation time was 210 s. In this case, the filament slid over a distance as long as 700 μm without showing a complete turn of the tail beads.

The observed fluctuations of the orientation of the bead-aggregate, relative to the actin filament, suggested that the range of rotational angular fluctuations was ~90° (i.e., ±45°) during the observation period of ~1 min (Fig. 5 *b*). This value was estimated by eye (and therefore is not precise) and represents four times the standard deviation, 4σ ($\pm 2\sigma$). The relatively small angular range might have resulted from steric hindrance (collision with the glass surface), particularly if the bead-aggregate had tended to rotate in a preferred direction. Therefore, in 25 filaments carrying double beads we examined

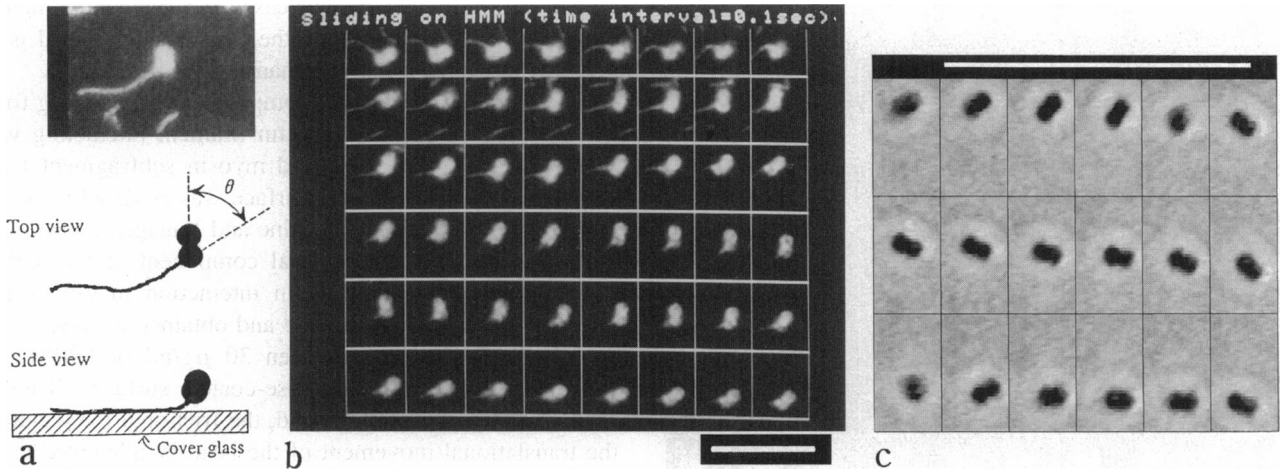

FIGURE 5 Images of a sliding double bead-tailed actin filament in the in vitro motility assay at 25°C (see Materials and Methods). (*a*) Fluorescence image of a sliding double bead-tailed actin filament and its schematic illustrations from the side and top. The diameter of each bead was 1.16 μm. The sliding speed was 4.0 μm/s. (*b*) A snapshot of the pulled double bead at 0.1-s intervals from left to right and top to bottom. If the double bead rotates around the actin filament, we can detect it as the change in the orientation of the bead-aggregate relative to the actin filament (θ in (*a*)). The snapshot shows that the range of angular fluctuations was ~90°. (*c*) A snapshot of phase contrast images, at 1/30-s intervals, of the double bead (bead diameter, 0.55 μm) pulled by an actin filament. The sequence, from left to right and top to bottom, shows a counterclockwise half turn followed by a clockwise half turn. Bars, 10 μm.

whether the second bead attached to the tail bead was located to the right or to the left of the sliding filament. In 8 of the 25 video sequences, the second bead predominantly resided on the right side. In 7, the second bead was on the left, and for the remaining 10, the second bead was found mainly on the filament axis (basically on top of the tail bead). Thus, collision of the second bead with the glass surface does not explain the small angular range, and it is not the reason why we failed to observe a complete turn of the bead-aggregate.

Hydrodynamic friction impedes the bead rotation in proportion to the cube of the bead radius (see Discussion). To reduce the friction, we tested beads with a diameter of 0.55 μm. Examination of 33 bead-tailed filaments, each for a continuous period of ~50 s, also failed to reveal a continuous rotation of the bead-aggregate. In the fluorescence images, however, it was difficult to ascertain whether a filament carried a double or a triple bead. Also, the orientation of the small bead-aggregate was not always unambiguous. Therefore, we observed seven bead-tailed filaments in phase-contrast images, in which double beads were clearly seen. Even in the phase images, the bead-aggregate went out of focus for a frame or two. Thus, the average unambiguous monitoring period was ~10 s. The double bead with the small diameter fluctuated considerably with an angular range of ≤180°. Occasionally, the bead-aggregate made a fast half turn. The fluctuations including such half turns, however, did not accumulate to make up a complete turn (Fig. 5 *c*).

Rotation of the tail beads relative to the actin filament

Although axial rotation in a sliding filament was observed as a superhelix by Nishizaka et al. (1993), we could not detect a complete turn of the bead-aggregate. One possible reason for the present result is that gelsolin (and the actin filament) was connected to the bead through only a single covalent bond around which the actin filament and the bead could rotate independently. To check this possibility, we observed rotational Brownian motion of bead-aggregates while the actin filaments were fixed on the glass surface through sparsely coated HMM in the rigor state. The sparse binding was achieved by perfusing a nitrocellulose-coated observation cell with an HMM solution at 0.3–3.0 μg/ml, 1/10–1/100 the concentration used in the motility assay (Nishizaka et al., 1995a). When bead-tailed actin filaments without ATP were introduced, the tail beads exhibited rotational Brownian motion whose amplitude depended on the length of the free actin tail. The range of angular fluctuations for an observation period of ~2 min was ~45° when the length of the filament between the bead surface and the first fixed point (HMM site) was ≤1 μm (n = 6), ~90° for 1–2 μm (n = 7), and ~180° for 3–4 μm (n = 4) (Fig. 6). This length dependence is consistent with the torsion of the free actin tail (see Discussion). Also, bead-aggregates at the tail never showed free rotational Brownian motion. Thus, we excluded the possibility of a single-bond linkage between gelsolin and the bead.

DISCUSSION

Bead-tailed actin filaments

Brown and Spudich (1979) reported that polylysine-coated polystyrene beads nucleated the polar assembly of G-actin to F-actin. They showed that the polarity of these filaments was uniform; the barbed end was away from the bead. Their preparation, however, was a multiple actin filament-bead

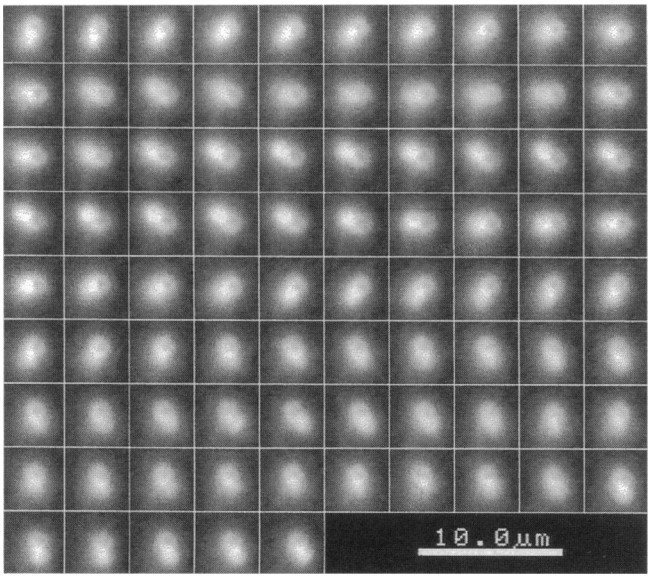

FIGURE 6 A snapshot of fluorescence images of rotational Brownian motion of a double bead at 2/30-s intervals from left to right and top to bottom. The actin filament was fixed on the glass surface through sparsely coated HMM in the rigor state. The length of the free actin filament tail (the length between the bead surface and the first fixed point) was ~3 μm. The range of the angular fluctuations was 180°; however, we never observed the free rotational motion of the bead-aggregate.

complex. They reported that the average number of filaments bound to a single bead was ~30 for the 1.1-μm beads and ~8 for the 0.1-μm beads (Brown and Spudich, 1981). In the present study, we succeeded in preparing a 1:1 polar complex of an actin filament with the gelsolin-coated bead. Our method may be applicable to the preparation of other types of polar complexes: for example, "bead-headed" actin filaments using pointed-end capping proteins such as a fraction of a β-actinin preparation (Funatsu et al., 1988), tropomodulin (Fowler et al., 1993), and so on (for a review see Pollard and Cooper, 1986). We tried DNase I (D4527; Sigma) as a candidate (Podolski and Steck, 1988) but failed in preparing a bead-headed actin filament; actin filaments did not bind to the DNase I-coated beads.

In vitro motility assay using bead-tailed actin filaments

To analyze the actomyosin motor force using bead-tailed actin filaments (Miyata et al., 1994, 1995), the bond between actin and gelsolin must be stronger than that force. Nishizaka et al. (1995b) measured the strength of a rigor bond between a bead-tailed actin filament and a single HMM molecule by pulling the tail bead with optical tweezers. The rigor bond was broken when pulled at 9.2 ± 4.4 pN, whereas the filament was not detached from the bead. This implies that the actin-gelsolin bond was stronger than 10 pN. In a similar experiment (T. Nishizaka, unpublished data) in which many myosin heads held an actin filament, the filament was detached from the bead at 49 ± 16 pN (n = 5), and in two cases the filament remained bound even at 70 pN. Thus, the actin-gelsolin bond is an order of magnitude stronger than a rigor bond.

The average translational component of the sliding force per micrometer of a single actin filament interacting with randomly oriented myosin and myosin subfragment-1 adsorbed on a silicone-coated surface was reported to be 9.6 and 5.4 pN, respectively (Kishino and Yanagida, 1988). We also measured the translational component of the sliding force produced by actomyosin interaction in our system using an optical trap technique and obtained a value of ~1 pN/μm of actin filament when 30 μg/ml of HMM was adsorbed on the nitrocellulose-coated surface (Kinosita et al., 1993). On the other hand, the frictional force against the translational movement of the bead is calculated using the Stokes equation: $F = 6\pi\eta r v$ (F, force; η, viscosity of the medium; r, radius of the bead; and v, sliding velocity). In the typical case in which a bead with a diameter of 1.16 μm is pulled at 4 μm/s, the frictional force is 0.044 pN. Thus, the frictional force is negligible compared with the translational component of the sliding force. This is consistent with the results in Fig. 3, in which the sliding velocity of the bead-tailed actin filaments was indistinguishable from that of nonbeaded actin filaments.

Torque for axial rotation of actin filament produced by actomyosin

A possible reason that continuous rotations of the bead-aggregates could not be detected is the hydrodynamic friction operating on them. The frictional moment against rotational motion of a single bead around its center is calculated by using the following equation: $N = 8\pi\eta r^3\omega$ (N, frictional torque on the single bead; η, viscosity of the medium; r, radius of the bead; ω, angular velocity) (Fig. 7 *a*). When another bead is bound to the side of the bead farthest from the rotational axis (Fig. 7 *c*), the frictional moment is ~5 × N, and this is the maximum frictional moment on a double bead. The frictional moment on a double bead is in the range 2 × N (Fig. 7 *b*) to 5 × N (Fig. 7 *c*). In the case in which double beads, each with a diameter of 1.16 μm, rotate at one turn per second, the range of required torque is calculated to be 62–154 pN · nm. In the case of 0.55-μm beads at the same speed, it is 6.6–16.0 pN · nm. The maximum diameter of an actin filament is estimated as 9–9.5 nm (Holmes et al., 1990). Therefore, at the surface of an actin filament, the rotational component of the sliding force that would produce the torque is 13–33 pN for the 1.16-μm beads and 1.4–3.5 pN for the 0.55-μm beads. The friction against rotation is significant compared with the translation because the torque has to be generated at the surface of the thin actin filament.

Rotation at one turn per second should be detected easily, yet we did not observe it even with the 0.55-μm beads. Therefore, we estimate that the rotational component of the sliding force and the torque produced on a sliding actin

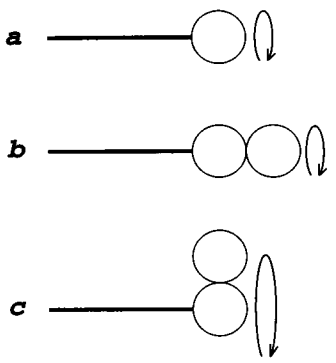

FIGURE 7 Hydrodynamic frictional moments against rotational motion of a double bead. The thick lines and open circles represent actin filaments and beads, respectively. (*a*) The frictional moment on a single bead is calculated using the equation $8\pi\eta r^3\omega$ (= *N*) (η, viscosity of the medium; r, radius of the bead; ω, angular velocity); (*b*), the minimum frictional moment on a double bead is calculated using the equation $2 \times 8\pi\eta r^3\omega$ (= 2*N*); and (*c*) the maximum frictional moment on a double bead is calculated using the equation $8\pi\eta r^3\omega + 8\pi\eta r^3\omega + 6\pi\eta r(2r)^2\omega$ (= 5*N*). The second and third terms of the latter equation show the contributions from the rotation and the translation of the outer bead, respectively. In the calculation for the double bead, we neglected the hydrodynamic interaction between the two beads.

filament (length $\leq$10 μm) in the present system of randomly oriented HMM lying on a nitrocellulose film without an external load did not accumulate >1 pN and 5 pN · nm, respectively.

We postulate that the torque produced by the sliding force accumulates with the torsion of the actin filament. After the torsional stress reaches a maximum, the actin-myosin interface slips, and the stress is released from the free front end of the sliding actin filament. The amount of torsion in a sliding filament is estimated as follows. The torsional rigidity of an actin filament has recently been estimated as $(2.6–3.7) \times 10^4$ pN · nm^2 from a normal-mode analysis of the atomic structure of F-actin (Ben-Avraham and Tirion, 1995). Direct observation of the torsional Brownian motion of F-actin has indicated similar values of $(2–10) \times 10^4$ pN · nm^2 (R. Yasuda, H. Miyata, and K. Kinosita, Jr., submitted for publication). The rotational Brownian motion of the tail beads observed in the present work also supports these values. Thus, the root mean squares of the torsional angular fluctuations $\Delta\gamma$ is related to the torsional rigidity C by $C(\Delta\gamma)^2/(2L) = k_BT$ in which L is the length of the filament and k_BT is the thermal energy (Barkley and Zimm, 1979). The angular range we report in this work is $4\Delta\gamma$, which is calculated for $C = 3 \times 10^4$ pN · nm^2 and $T = 298$ K as 84°, 120°, and 168° for $L = 1$ μm, 2 μm, and 4 μm, respectively. The observed values of 45°, 90°, and 180° are in accord with the expected values when limited precision is taken into account. For $C = 3 \times 10^4$ pN · nm^2, the estimated maximal torque of 5 pN · nm above would twist an actin filament with a length of 10 μm by a quarter of a turn (Barkley and Zimm, 1979). Thus, a sliding filament is unlikely to contain a large torsional strain.

The superhelix observed by Tanaka et al. (1992) and the supercoil observed by Nishizaka et al. (1993) indicated that an actin filament was twisted one turn and more than three turns, respectively. The accumulated torsional stress on the actin-myosin interface may not be very high, however, because it will be released by the formation of the superhelix and the supercoil. Therefore, we conclude that these observations are not inconsistent with the present result.

The last important point we must consider is that the sliding force depends on the load. The reason we did not detect the rotational motion of the actin filament may be concerned with this point. In the experiments performed by Nishizaka et al. (1993) and Tanaka et al. (1992), the observed actin filament slid under a translationally loaded condition because the sliding of the front part of it was stopped or reduced. In our system, however, bead-tailed actin filaments slid without a translational load, as indicated by the small translational friction estimated above and shown in Fig. 3. Under a loaded condition, actomyosin produces more sliding force, and its torque might be accumulated more efficiently.

Our results do not deny the axial rotation in the sliding actin filament, but they show that forward movement occurs at the same speed as that of a nonbeaded actin filament even when a large axial torque load is imposed by the hydrodynamic friction. Also, in the case of a microtubule and 14S dynein, Vale and Toyoshima (1988) reported that forward movement occurred even when rotation was suppressed by steric interference. These observations that the translocation and the rotation are not tightly coupled offer an important key for understanding the sliding mechanism.

This study was supported in part by a Grant-in-aid for the Encouragement of Young Scientists and by Grants-in-aid for the General Scientific Research from the Ministry of Education, Science and Culture of Japan, and in part by Special Coordination Funds for Promoting Science and Technology from the Agency of Science and Technology of Japan.

REFERENCES

Ashkin, A. 1992. Forces of a single-beam gradient laser trap on a dielectric sphere in the ray optics regime. *Biophys. J.* 61:569–582.

Barkley, M. D., and B. H. Zimm. 1979. Theory of twisting and bending of chain macromolecules: analysis of the fluorescence depolarization of DNA. *J. Chem. Phys.* 70:2991–3007.

Ben-Avraham, D., and M. M. Tirion. 1995. Dynamic and elastic properties of F-actin: a normal-modes analysis. *Biophys. J.* 68:1231–1245.

Block, S. M., and K. Svoboda. 1995. Analysis of high resolution recordings of motor movement. *Biophys. J.* 68:230s–241s.

Brown, S. S., and J. A. Spudich. 1979. Nucleation of polar actin filament assembly by a positively charged surface. *J. Cell Biol.* 80:499–504.

Brown, S. S., and J. A. Spudich. 1981. Mechanism of action of cytochalasin: evidence that it binds to actin filament ends. *J. Cell Biol.* 88:487–491.

Coppin, C. M., J. T. Finer, J. A. Spudich, and R. D. Vale. 1995. Measurement of the isometric force exerted by a single kinesin molecule. *Biophys. J.* 68:242s–244s.

Ebashi, S., and K. Maruyama. 1965. Preparation and some properties of α-actinin-free actin. *J. Biochem. (Tokyo).* 58:20–26.

Finer, J. T., A. D. Mehta, and J. A. Spudich. 1995. Characterization of single actin-myosin interactions. *Biophys. J.* 68:291s–297s.

Finer, J. T., R. M. Simmons, and J. A. Spudich. 1994. Single myosin molecule mechanics: piconewton forces and nanometre steps. *Nature (Lond.).* 368:113–119.

Fowler, V. M., M. A. Sussmann, P. G. Miller, B. E. Flucher, and M. P. Daniels. 1993. Tropomodulin is associated with the free (pointed) ends of the thin filaments in rat skeletal muscle. *J. Cell Biol.* 120:411–420.

Funatsu, T., Y. Asami, and S. Ishiwata. 1988. β-actinin: a capping protein at the pointed end of thin filaments in skeletal muscle. *J. Biochem. (Tokyo).* 103:61–71.

Funatsu, T., H. Higuchi, and S. Ishiwata. 1990. Elastic filaments in skeletal muscle revealed by selective removal of thin filaments with plasma gelsolin. *J. Cell Biol.* 110:53–62.

Gelles, J., B. J. Schnapp, and M. P. Sheetz, 1988. Tracking kinesin-driven movements with nanometer-scale precision. *Nature (Lond.).* 331: 450–453.

Harada, Y., K. Sakurada, T. Aoki, D. D. Thomas, and T. Yanagida. 1990. Mechanochemical coupling in actomyosin energy transduction studied by in vitro movement assay. *J. Mol. Biol.* 216:49–68.

Holmes, K. C., D. Popp, W. Gebhard, and W. Kabsch. 1990. Atomic model of the actin filament. *Nature (Lond.).* 347:44–49

Holtzer, A., and S. Lowey. 1959. The molecular weight, size and shape of the myosin molecule. *J. Am. Chem. Soc.* 81:1370–1377.

Houk, Jr., T. W., and K. Ue. 1974. The measurement of actin concentration in solution: a comparison of methods. *Anal. Biochem.* 62:66–74.

Huxley, H. E. 1990. Sliding filaments and molecular motile systems. *J. Biol. Chem.* 265:8347–8350.

Isenberg, G. 1991. Actin binding proteins-lipid interaction. *J. Muscle Res. Cell Motil.* 12:136–144.

Kinosita, Jr., K., N. Suzuki, S. Ishiwata, T. Nishizaka, H. Itoh, H. Hakozaki, G. Marriott, and H. Miyata. 1993. Orientation of actin monomers in moving actin filaments. *In* Mechanism of Myofilament Sliding in Muscle Contraction. H. Sugi and G. H. Pollack, editors. Plenum Publishing, New York. 321–329.

Kishino, A., and T. Yanagida. 1988. Force measurements by micromanipulation of a single actin filament by glass needles. *Nature (Lond.).* 334:74–76.

Kron, S. J., Y. Y. Toyoshima, T. Q. P. Uyeda, and J. A. Spudich. 1991. Assays for actin sliding movement over myosin-coated surfaces. *Methods Enzymol.* 196:399–416.

Kuo, S. C., and M. P. Sheetz. 1993. Force of single kinesin molecules measured with optical tweezers. *Science.* 260:232–234.

Kurokawa, H., W. Fujii, K. Ohmi, T. Sakurai, and Y. Nonomura. 1990. Simple and rapid purification of brevin. *Biochem. Biophys. Res. Commun.* 168:451–457.

Margossian, S. S., and S. Lowey. 1978. Interaction of myosin subfragments with F-actin. *Biochemistry.* 17:5431–5439.

Miyata, H., H. Hakozaki, H. Yoshikawa, N. Suzuki, K. Kinosita, Jr., T. Nishizaka, and S. Ishiwata. 1994. Stepwise motion of an actin filament over a small number of heavy meromyosin molecules is revealed in an in vitro motility assay. *J. Biochem. (Tokyo).* 115:644–647.

Miyata, H., H. Yoshikawa, H. Hakozaki, N. Suzuki, T. Furuno, A. Ikegami, K. Kinosita, Jr., T. Nishizaka, and S. Ishiwata. 1995. Mechanical measurements of single actomyosin motor force. *Biophys. J.* 68:286s–290s.

Molloy, J. E., J. E. Burns, J. C. Sparrow, R. T. Tregear, J. Kendrick-Jones, and D. C. S. White. 1995. Single-molecule mechanics of heavy meromyosin and S1 interacting with rabbit or *drosophila* actins using optical tweezers. *Biophys. J.* 68:298s–305s.

Nishizaka, T., H. Miyata, H. Yoshikawa, S. Ishiwata, and K. Kinosita, Jr. 1995a. Mechanical properties of single protein motor of muscle studied by optical tweezers. *Biophys. J.* 68:75s.

Nishizaka, T., H. Miyata, H. Yoshikawa, S. Ishiwata, and K. Kinosita, Jr. 1995b. Unbinding force of a single motor molecule of muscle measured using optical tweezers. *Nature (Lond.).* 377:251–254.

Nishizaka, T., T. Yagi, Y. Tanaka, and S. Ishiwata. 1993. Right-handed rotation of an actin filament in an in vitro motile system. *Nature (Lond.).* 361:269–271.

Perry, S. V. 1955. Myosin adenosine triphosphatase. *Methods Enzymol.* 2:582–588.

Podolski, J. L., and T. L. Steck. 1988. Association of deoxyribonuclease I with the pointed ends of actin filaments in human red blood cell membrane skeletons. *J. Biol. Chem.* 263:638–645.

Pollard, T. D., and J. A. Cooper. 1986. Actin and actin-binding proteins. A critical evaluation of mechanisms and functions. *Annu. Rev. Biochem.* 55:987–1035.

Saito, K., T. Aoki, T. Aoki, and T. Yanagida. 1994. Movement of single myosin filaments and myosin step size on an actin filament suspended in solution by a laser trap. *Biophys. J.* 66:769–777.

Spudich, J. A., and S. Watt. 1971. The regulation of rabbit skeletal muscle contraction. I. Biochemical studies of the interaction of the tropomyosin-troponin complex with actin and the proteolytic fragments of myosin. *J. Biol. Chem.* 246:4866–4871.

Svoboda, K., and S. M. Block, 1994. Force and velocity measured for single kinesin molecules. *Cell.* 77:773–784.

Svoboda, K., C. F. Schmidt, B. J. Schnapp, and S. M. Block. 1993. Direct observation of kinesin stepping by optical trapping interferometry. *Nature (Lond.).* 365:721–727.

Tanaka, Y., A. Ishijima, and S. Ishiwata. 1992. Super helix formation of actin filaments in an in vitro motile system. *Biochim. Biophys. Acta.* 1159:94–98.

Vale, R. D. 1994. Getting a grip on myosin. *Cell.* 78:733–737.

Vale, R. D., and L. S. B. Goldstein. 1990. One motor, many tails: an expanding repertoire of force-generating enzymes. *Cell.* 60:883–885.

Vale, R. D., and Y. Y. Toyoshima. 1988. Rotation and translocation of microtubules in vitro induced by dyneins from tetrahymena cilia. *Cell.* 52:459–469.

Weber, A., M. Pring, S.-L. Lin, and J. Bryan. 1991. Role of the N- and C-terminal actin-binding domains of gelsolin in barbed filament end capping. *Biochemistry.* 30:9327–9344.

Weeds, A. G., and R. S. Taylor. 1975. Separation of subfragment-1 isoenzymes from rabbit skeletal muscle myosin. *Nature (Lond.).* 257: 54–56.

Yanagida, T., and A. Ishijima. 1995. Forces and steps generated by single myosin molecules. *Biophys. J.* 68:312s–320s.

Yanagida, T., Y. Harada, and A. Ishijima. 1993. Nano-manipulation of actomyosin molecular motors in vitro: a new working principle. *Trends Biochem. Sci.* 18:319–324.

Yanagida, T., M. Nakase, K. Nishiyama, and F. Oosawa. 1984. Direct observation of motion of single F-actin filaments in the presence of myosin. *Nature (Lond.).* 307:58–60.